STRESS CORROSION CRACKING OF AA5083 (Al-4.5Mg-1.0Mn)

[1]J.L. Searles, [2]P.I. Gouma, and [3]R.G. Buchheit
Fontana Corrosion Center
Department of Materials Science and Engineering
Ohio State University
Columbus, Ohio 43210

ABSTRACT

AA5083 (Al-4.4Mg-0.7Mn-0.15Cr) is a non-heat treatable alloy that is generally known for its excellent corrosion resistance. However, it can become susceptible to stress corrosion cracking (SCC) when exposed to temperatures ranging from 50^o to 200^{o}C. This is widely believed to be due to dissolution of the electrochemically active β phase, Al_3Mg_2, precipitated on grain boundaries. More recently, alternative mechanisms have been invoked related to hydrogen effects and/or free Mg segregation or depletion in the grain boundary regions. To establish a proper baseline for the sensitization effect, and to aid in resolving mechanistic uncertainties, constant extension rate testing (CERT) was conducted on sensitized samples under open circuit conditions and under potential control. Tests conducted in 3.5% NaCl at open circuit showed a strong dependence on heat treatment time, with SCC resistance at a minimum at 189 hours, followed by a slight increase at longer times. The measured open circuit potential during the tests was consistently above the β breakaway potential determined in earlier experiments. Further CERT evaluation focused on testing at an applied potential, -980mV$_{SCE}$, below the observed β breakaway potential, -910mV$_{SCE}$. Under potential control, samples representing all degrees of β precipitation from 82.5 to 333 hours regained the full ductility that was observed in air tests. These findings strongly support the classical anodic dissolution mechanism originally proposed to explain SCC in these alloys.

[1] Currently at Procter and Gamble, 6250 Center Hill Ave., Cincinnati, OH 45224.
[2] Currently at the Department of Materials Science and Engineering, State University of New York at Stony Brook, Stony Brook, NY 11794
[3] Corresponding author: 477 Watts Hall, 2014 College Rd. Columbus, Ohio 43210

INTRODUCTION

AA 5083 (Al-4.5mg-1.0Mn) is a medium strength, non-heat treatable alloy that is generally known for its excellent corrosion resistance. However, it can become susceptible to stress corrosion cracking (SCC) when exposed to temperatures ranging from 50^{o} to 200^{o}C for sufficiently long periods of time. This phenomenon is known as "sensitization" and is widely associated with the precipitation of β phase (Al_3Mg_2) on grain boundaries.

Early work on Al-Mg alloys attributed intergranular attack (IGA) and stress corrosion cracking (SCC) of sensitized Al-Mg alloys to selective anodic dissolution of β precipitates from grain boundaries (1). This theory explains the experimental observation that when grain boundaries are free of β, IGA and SCC do not occur. However, when sensitization leads to continuous lining of the grain boundaries, both forms of attack are severe. Certain sensitization treatments lead to discontinuous β precipitation on boundaries. In this case, alloys may or may not show evidence of IGA, and are usually only moderately susceptible to SCC (1). Recently, mechanisms involving hydrogen embrittlement and Mg-depleted zones have been proposed. While the details of each theory are not presented here, it is evident that the degree of β precipitation on the grain boundaries lies at the heart of each and appears to be essential for the initiation of stress corrosion cracks.

EXPERIMENTAL PROCEDURES

Repassivation

Repassivation kinetics for 5083 and bulk synthesized β were measured by a scratch technique using a Nicolet Pro34 oscilloscope. Samples were immersed in 3.5% NaCl for 20 minutes to obtain a stable OCP. The sample was polarized to -980mV_{SCE} and held for 10 minutes with the PAR 263A potentiostat. Scratching was performed at -980mV_{SCE} with a sharp alumina rod. The changes in current were measured at a sweep frequency of 50μs in the current range of 100μA and 10μA until it decayed to a minimum.

Constant Extension Rate (CER) Testing

Sample Preparation and Test Apparatus. Tensile samples were prepared from 6mm thick 5083 sheet such that the load axis was transverse to the rolling direction. Tensile sample blanks were sensitized at 150^{o}C for times up to 333 hours. The as-machined gage length was ground from 600 to 1200 grit sandpaper to obtain a uniform surface before each test. Each bar was degreased in ethanol and dried before attaching the grips. For tests in solution, the interface between the sample and the grip was coated with microstop to protect the grip and prevent crevice corrosion that might cloud the results of the test.

The M-CERT^{TM} test system was used to apply a constant extension rate to the sample. The frame had a load capacity of 10,000lbs and a maximum stroke of 2in (2). It was assumed that all the measured displacement took place in the gage length of the tensile sample, with negligible contributions from the 316 stainless steel load frame. A glass cell was used to perform environmental CER tests. The approximate volume to specimen surface area ratio was ≥ 30mL/cm (2).

Test Conditions. All tests were conducted at an extension rate of 10^{-6}in/s with an initial load of about 90 lbs. As a baseline, all samples were tested in lab air first. Strain to failure based on the original gage length was used as a figure of merit for comparing the effect of sensitization heat treatment and environment on the mechanical properties. Since there was no systematic variation in mechanical properties in air as a function of sensitization time, the average displacement, excluding the high and low, was used to normalize the environmental data.

The second batch of testing was conducted on solution heat-treated (SHT) and sensitized 5083 in 3.5% NaCl under open circuit conditions. The open circuit potential was measured during the test using a Gamry PC3-4 potentiostat. OCP data for the duration of the CER test was collected at 0.2 points/sec in 24 hour segments. Some OCP data was collected at a faster rate of 5 points/sec to observe spikes in the potential as cracking proceeded in the later stages of the test.

Based on the electrochemical data collected for 5083 and β, presented elsewhere (3, 4), the next step was to test in 3.5% NaCl under potential control to -980mV_{SCE}, which is below the β breakaway potential. The current was measured under these conditions at a rate of 0.14 points/sec. The potential was not interrupted for the duration of the CER test.

All these tests were also conducted on as-received cold-rolled 5083 sheet. Although the exact condition of the plate is unknown, a common mill condition is only about 18% cold work (CW) in addition to some hot working. A comparison of the short transverse grain size between SHT and CW samples did not show a dramatic difference to suggest that this plays a role in SCC behavior. These samples were polished to 1μm alumina finish and etched with a modified Poulton's reagent containing 12mL HCl (conc), 16mL HNO_3 (conc), 1mL HF (48%), 1mL H_2O, and 16mL of a solution consisting of 3g chromic acid per 10mL H_2O (5).

Additional tests on SHT and sensitized samples were conducted in humid air in order to study possible hydrogen effects on SCC behavior. Saturated NH_4Cl maintained at 25-30°C was placed in the bottom of the cell, out of contact with the sample, to produce a relative humidity of 77.5-79.3% inside the closed cell (6).

Transmission Electron Microscopy

Sample Preparation. Transmission electron microscopy (TEM) was used to assess the degree of β precipitation on the grain boundaries as a function of sensitization time. TEM foils were prepared from samples sensitized for 9, 82.5, 189, 262, and 333 hours at 150°C. Disks were cut from the threaded region of tensile specimens on a slow speed diamond saw and thinned to 150μm with 600 grit sandpaper. 3mm disks were punched, dimpled, and ion milled using an Ar gun at 6kV and 1mA with a milling angle <12° until perforation.

Sample Examination. Two TEM systems were utilized for analysis of sensitized samples. Phase analysis of grain boundary precipitates was conducted using a Philips CM200 TEM. This machine uses a LaB_6 filament operating at 200kV. It is also equipped with energy dispersive x-ray spectroscopy (EDXS) to analyze the composition of precipitates. Bright field and dark field images were taken to illustrate phase distribution. In addition, diffraction analysis was used for phase identification. Further analysis of elemental distribution around grain boundaries and precipitates was conducted on a Philips CM300 FEG TEM. This is a field emission gun (FEG) TEM operating at 300kV. It has scanning transmission electron microscopy (STEM) capabilities in addition to conventional TEM and EDXS analysis. STEM was used in conjunction with the EMISPEC™ software program for elemental mapping and line profiling in the vicinity of the grain boundaries to identify precipitates and assess the depletion or segregation of Mg.

RESULTS AND DISCUSSION

Repassivation

Repassivation kinetics for AA5083 and bulk synthesized β were measured using the scratch technique in aerated 3.5% NaCl. At the open circuit potential of 5083, approximately $-740mV_{SCE}$, both the alloy and β are active so the scratch did not repassivate, but continued to dissolve. In fact, dissolution of β occurred over the entire surface of the sample at this potential, even in the absence of scratching.

Under polarization conditions to $-980mV_{SCE}$, which is below the breakaway potential of β, repassivation behavior is much different. Both samples at this potential are in their respective passive regions, so repassivation of the scratch is expected. Figure 1 shows the repassivation transients measured for each sample at this potential. The data have been normalized to the highest current value, 0.134mA, to account for the difference in area of the scratches. The area under each curve represents the amount of material corroded before repassivation of the scratch. The time for repassivation of the 5083 scratch was 0.40 sec, while β repassivated in only 0.16 sec. This data indicates that below the breakaway potential of β, the alloy repassivates slower than β. In addition, while the polarization data, presented in previous work, indicates that the steady state current after repassivation is on the order of $100\mu A/cm^2$, the result of the scratching experiment suggests that β is truly passive in this potential region. The implications of this result will be discussed below regarding constant extension rate testing (CERT).

TEM Evaluation

TEM techniques were used to investigate the degree of grain boundary β precipitation, which was correlated to CERT results discussed below. A short 9 hour sensitization treatment produced one very small, isolated β precipitate visible in the TEM foil. The rest of the grain boundary structure was either precipitate-free or decorated by Al_6Mn precipitates as confirmed by EDS. This microstructure represents a resistant condition. However, with longer sensitization times, β precipitation increases, leading to a more susceptible condition. The sample sensitized for 82.5 hours showed slight grain boundary precipitation in the form of discreet particles separated by micrometer distances. The precipitate shown in the bright field image in Figure 2 was identified as β through analysis of the diffraction pattern shown in the inset. In addition to diffraction analysis, elemental mapping of the particles using the STEM imaging mode and the EMISPEC™ software confirmed the chemical nature of the particles.

After 189 hours at 150°C, a continuous film was formed, which is shown in bright field over several micrometers of grain boundary in Figure 3. This microstructure represents the most susceptible condition as discussed below. Further sensitization for 262 hours coarsened the precipitate to form large discreet particles along the boundary. Further precipitation after a longer time of 333 hours resulted in a semi-continuous film that again increased SCC susceptibility.

CER Testing

Air. CER tests were first conducted in air to obtain a baseline for comparison with environmental tests. SHT samples from every sensitization period were tested in air, and it was found that there was no significant variation in mechanical properties (Figure 4). The average strain to failure used to normalize SHT environmental tests was 0.209, while the average yield stress and maximum stress were 140MPa and 350MPa, respectively. This result supports earlier work that also showed no variation in the mechanical properties of 5XXX alloys in air as a function of sensitization time (7). It is also clear that the mechanical properties of β, or any depleted region associated with its precipitation, do not affect the overall performance of the alloy in the absence of a corrosive environment, even when a continuous film or region is present.

3.5% NaCl at OCP. Sensitized samples were tested in 3.5% NaCl under free corrosion conditions. Samples sensitized for 0, 9, and 45 hours showed no loss in ductility. At 82.5 hours, the ductility had decreased by 50% followed by further decreases at 164 hours and finally to a minimum of 5.5% total elongation at 189 hours, which is only 26% of the ductility in air. Ductility was shown to increase again to 12.8% at 262 hours followed by another decrease at 333 hours. This behavior is shown in Figure 5. The yield stress remained unchanged during these tests relative to the air tests. The OCP collected at a slow rate of 0.2pts/sec during all tests was between $-800mV_{SCE}$ and $-900mV_{SCE}$.

TEM evaluation regarding the evolution of grain boundary β precipitation correlates with ductility as a function of sensitization time under free corrosion conditions (Figure 5). As β begins to precipitate discontinuously on the grain boundaries, shown after 82.5 hours, the ductility drops. With increased grain boundary lining, ductility continues to decrease until a minimum is reached after 189 hours where a continuous film is formed. The recovery observed after 262 hours is also supported by TEM results showing discreet β present as larger particles due to coarsening of the precipitate with increased time. After still longer times, the precipitate film becomes semi-continuous again as β continues to precipitate, and the ductility decreases again.

The combination of CERT results and TEM evaluation directly supports the anodic dissolution mechanism of SCC. In addition to this evidence, the measured OCP both in deaerated conditions and at 0.2pts/sec during CER tests was always above the measured breakaway potential for β in the pH range 6-8, $-940mV_{SCE}$. The anodic polarization of β in this environment stimulates rapid anodic dissolution from the grain boundaries where it has primarily precipitated, causing cracking. Therefore, the electrochemical characteristics of the system also strongly support the anodic dissolution mechanism of attack.

3.5% NaCl at $-980mV_{SCE}$. Further evidence in support of the anodic dissolution mechanism of SCC results from CER tests conducted at $-980mV_{SCE}$. This potential was chosen because it was below the β breakaway potential of $-940mV_{SCE}$, but not low enough to induce significant cathodic corrosion that would obscure its effect on β dissolution. It was observed that, under potential control, over 90% of the ductility was recovered for all samples (Figure 6). All but one recovered 100% ductility relative to the average used to normalize the results, 0.209. The remaining sample at 164 hours recovered 98% of its individual ductility measured in air, 0.189 out of 0.193, but was still 10% below the average for the range.

SCC is shut off by electrochemical polarization below the β phase breakaway potential. Since selective β phase dissolution was eliminated under these conditions, SCC did not occur, even in the most susceptible condition, sensitized for 189 hours with continuous grain boundary lining. This evidence strongly implicates anodic dissolution as the primary factor in SCC of this alloy in near-neutral chloride solutions, and suggests that HE plays no more than a minor role in the cracking process. Were HE playing a larger role in SCC, the 200mV cathodic polarization in the CER experiment conducted under potential control might be expected to increase the hydrogen fugacity near the sample surface and promote susceptibility to cracking slightly. Clearly this is not the case. Regarding the Mg depletion mechanism, cathodic polarization would not drastically affect the failure through this region since the overall electrochemical nature of the region is not much different than in the matrix. Although β dissolution is necessary for the removal of the mechanical constraint according to this mechanism, evidence of intergranular crack initiation at the grain boundaries that were not constrained by β and which originated on the surface of the tensile sample was not observed under polarization conditions. Therefore, this experimental CERT evidence at $-980mV_{SCE}$ strongly supports anodic dissolution of β as the primary contributor to SCC of sensitized AA5083.

Fractography

Air. The fracture surfaces from tensile samples tested in air showed no variation in characteristics across the sensitization range from 0 hours to 333 hours. Figure 7 shows a typical fracture surface consistent with ductile overload failure.

3.5% NaCl at OCP and -980mV$_{SCE}$. The amount of intergranular corrosion evident on the fracture surface of the CERT tensile samples increases as strain to failure decreases and degree of grain boundary precipitate lining increases. This trend is evident regardless of the environment, 3.5% NaCl or 78% relative humidity.

In 3.5% NaCl at OCP, those sensitization times that maintained 100% ductility, 9 hours and 45 hours, also maintained the characteristic ductile overload fracture surface. With increased β precipitation after 82.5 hours, the strain to failure decreased, and intergranular attack is observed at crack initiation sites. With the high degrees of grain boundary precipitation and minimum SCC resistance after sensitizing for 164 hours and 189 hours, intergranular attack is observed over half of the fracture surface (Figure 8). Even the increase in ductility due to coarsening of β precipitates after 262 hours is evident in a decreased intergranular attack area on the fracture surface. After sensitizing for 333 hours, a greater degree of intergranular attack is again observed. With all samples, when the remaining cross sectional area is too small to support the applied load, the sample undergoes ductile overload similar to failure in air.

In contrast to intergranular failure under free corrosion conditions, tensile samples polarized to -980mV$_{SCE}$ during testing failed by ductile overload, just as those tested in air did. This type of failure is again shown in Figure 9 for the most susceptible condition after 189 hours, which produced a continuous β film on the grain boundaries.

Comments on the Anodic Dissolution Mechanism

The results of this study permit two comments to be made on the anodic dissolution-based SCC mechanism as it has been described in the literature (1, 8). First, the original presentations of the mechanism suggested that SCC in sensitized alloys can be shut down when the potential of the alloy is lowered to or below that of the β phase open circuit potential. Under the environmental conditions examined here, the β phase open circuit potential is about -1250mV$_{SCE}$ (3, 4). In the absence of polarization data for β, the original mechanism could not account for the spontaneous passivity of β. In fact, these new results show that the alloy need only be polarized below the β breakaway to suppress dissolution. In these environments, that potential is about -940mV$_{SCE}$. This difference may be important when considering iR effects on crack growth rates.

Second, Sprowls and Brown (1) suggested that intragranular precipitation of β would have a beneficial effect on SCC resistance since the galvanic driving force for grain boundary β dissolution would be lowered. These and related results (3, 4) indicate that any substantive positive effect of intragranular β precipitation is unlikely in near neutral chloride solutions. This is so because the open circuit potential of the alloy is always much more positive that the β breakaway potential, even in deaerated solutions, and since β is spontaneously passive, it is easily polarized to (and past) is breakaway potential.

CONCLUSIONS

Major Observations

The SCC susceptibility of sensitized AA5083 was investigated using a combination of techniques, including primarily TEM, CERT, and SEM fractography. Based on the results obtained from these techniques, the following major observations were made:

- Total strain to failure in 3.5% NaCl under free corrosion conditions during CER tests reaches a minimum after a 189 hour sensitization heat treatment at 150°C, followed by an increase and possibly a further decrease after longer times.

- Grain boundary β precipitation forms a continuous film after 189 hour sensitization heat treatment at 150°C.

- Grain boundary β precipitates coarsen and then become semi-continuous again after longer times.

- Degree of intergranular attack increases with sensitization time to reach a maximum after 189 hours.

- Cathodic polarization to -980mV_{SCE}, which is below the β breakaway potential, inhibits SCC in 3.5% NaCl.

Significance

SCC in 5XXX alloys was first explained in terms of the simple anodic dissolution model that accounted for much of the phenomenology of Al-Mg SCC. Recently, other ideas regarding hydrogen effects and Mg depletion or segregation have attempted to explain the SCC behavior of this alloy system. However, this work shows that SCC susceptibility scales directly with the degree of grain boundary β precipitation, regardless of which mechanism is at play, and that the original anodic dissolution model is sufficient in accounting for the SCC behavior of AA5083.

ACKNOWLEDGMENTS

The authors would like to thank Ryan Leard for providing bulk Al_3Mg_2 and $MgZn_2$ phases for study. This work was supported by Pechiney Rolled Products and the Department of Energy office of Basic Energy Sciences Center for Synthesis and Processing in a grant through Sandia National Laboratories, Albuquerque, New Mexico.

REFERENCES

1. D.O. Sprowls and R.H. Brown, in *Fundamental Aspects of Stress Corrosion Cracking*, R.W. Staehle, A.J. Forty, editors, p. 466, National Association of Corrosion Engineers, Houston, TX (1969).

2. M-CERT™ Test System User's Manual, Intercorr International, Inc., Houston, TX, 1999.

3. J.L. Searles, "The Electrochemical Characteristics of Al_3Mg_2 and Stress Corrosion Cracking of AA5083" M.S. Thesis, Ohio State University (2000).

4. J.L. Searles, R.M. Leard, R.G. Buchheit, submitted to *Metall. Trans.* Sept. 2000.

5. *ASM Handbook*, **9**, p.352, ASM International, Metals Park, OH (1995).

6. R.C. Weast, ed., *CRC Handbook of Chemistry and Physics 67th ed.*, p. E42, CRC Press, Boca Raton, FL (1987).

7. T. Mae, M. Ihara, K. Komura, S. Toriyama, S. Sunada, and K. Arai, *Mater. Trans. JIM*, **37**, 1781 (1996).

8. R.B. Mears, R.H. Brown, and E.H. Dix, Jr., *in Symposium on Stress Corrosion Cracking of Metals*, p.329, ASTM and AIME (1944).

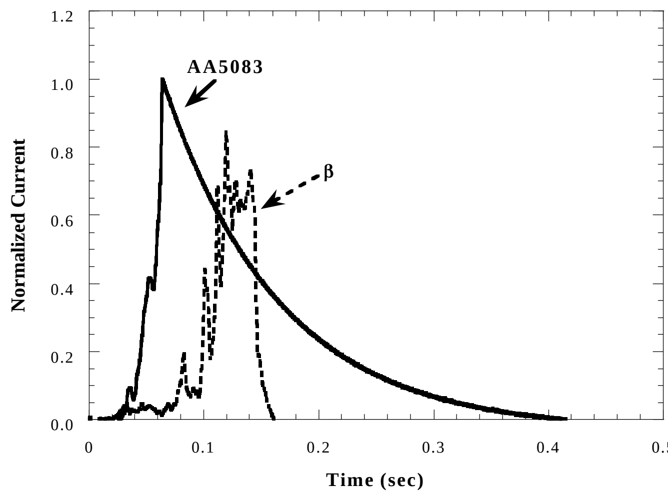

Figure 1: Repassivation transient of β and 5083 after scratching in aerated 3.5% NaCl.

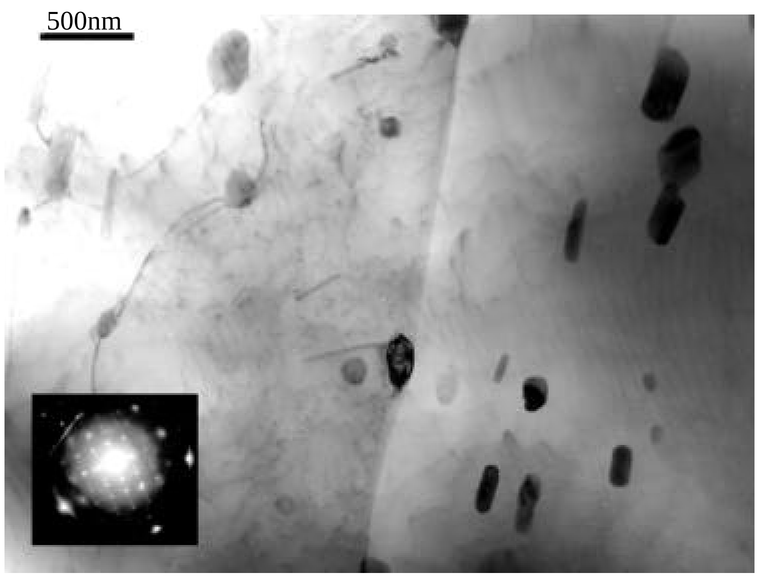

Figure 2: TEM micrograph of 82.5 hour sample showing discreet β precipitates on grain boundaries with associated diffraction pattern along the <110> zone axis.

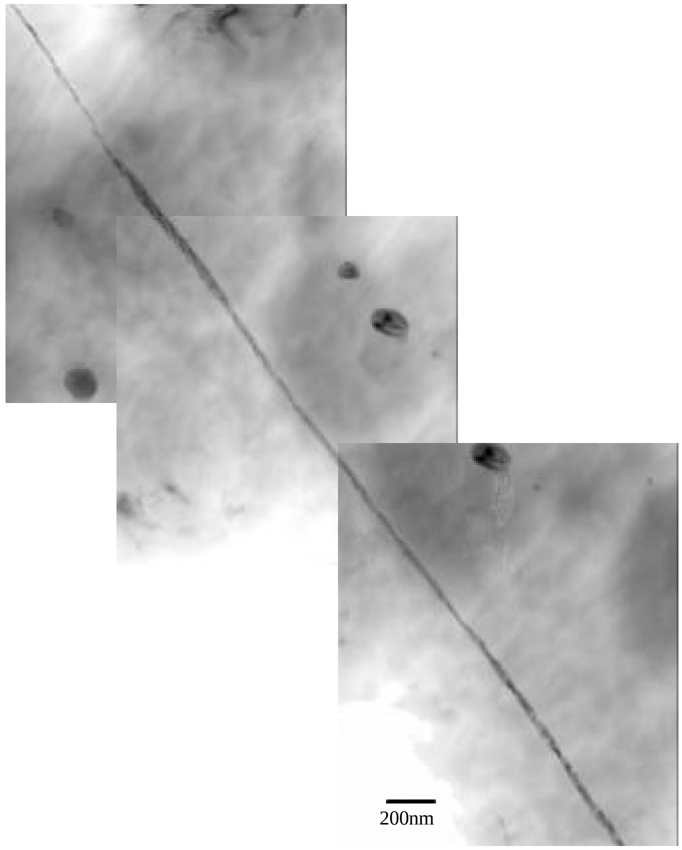

Figure 3: TEM composite micrograph of 189 hour sample showing continuous β film lining the grain boundaries.

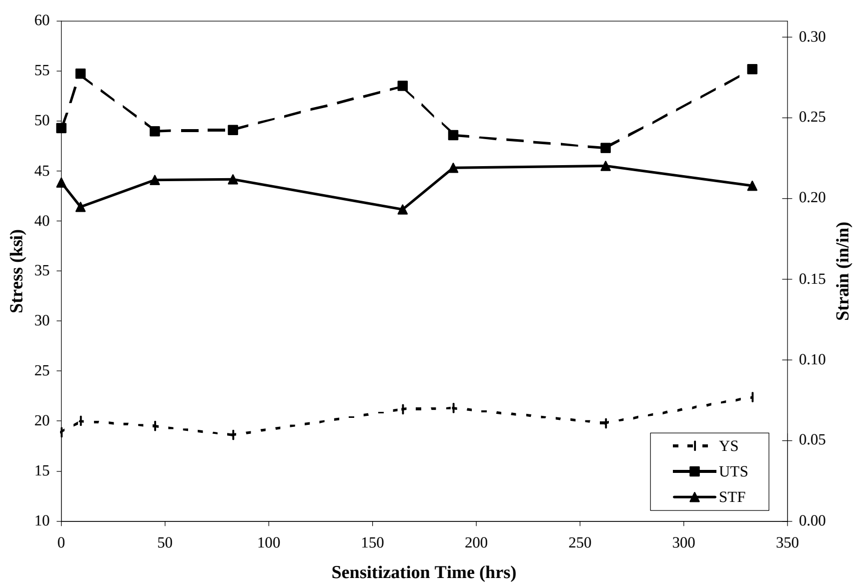

Figure 4: Mechanical properties measured in air for AA5083 as a function of sensitization time.

Keywords:

Al-Mg alloys, AA5083, Stress Corrosion Cracking, Al_3Mg_2, Constant Extension Rate Testing, Anodic Dissolution, Environmental Fracture.